Heterologous overexpression and characterization of a flavoprotein-cytochrome *c* complex fructose dehydrogenase of *Gluconobacter japonicus* NBRC3260

Shota Kawai[1], Maiko Goda-Tsutsumi[1], Toshiharu Yakushi[2]*, Kenji Kano[1], and Kazunobu Matsushita[2]

[1]Division of Applied Life Sciences, Graduate School of Agriculture, Kyoto University, Sakyo-ku, Kyoto 606-8502, Japan; [2]Department of Biological Chemistry, Faculty of Agriculture, Yamaguchi University, Yamaguchi 753-8515, Japan

Running title: Expression of the *fdhSCL* genes of *Gluconobacter* sp.

*To whom correspondence should be addressed: Toshiharu Yakushi, Department of Biological Chemistry, Faculty of Agriculture, Yamaguchi University, Yamaguchi 753-8515, Japan, Tel: +81-83-933-5857, Fax: +81-83-933-5859, E-mail: juji@yamaguchi-u.ac.jp

Abstract

A heterotrimeric flavoprotein-cytochrome *c* complex fructose dehydrogenase (FDH) of *Gluconobacter japonicus* NBRC3260 catalyzes the oxidation of D-fructose to produce 5-keto-D-fructose and is used for diagnosis and basic research purposes as a direct electron transfer-type bioelectrocatalysis. The *fdhSCL* genes encoding the FDH complex of *G. japonicus* NBRC3260 were isolated by a PCR-based gene amplification method with degenerate primers designed from the amino terminal amino acid sequence of the large subunit and sequenced. Three open reading frames for *fdhSCL* encoding the small, cytochrome *c,* and large subunits, respectively, were found and presumably in a polycistronic transcriptional unit. Heterologous overexpression of *fdhSCL* was conducted using a broad host range plasmid vector pBBR1MCS-4 carrying a DNA fragment containing the putative promoter region of the membrane-bound alcohol dehydrogenase gene of *Gluconobacter oxydans* and a *G. oxydans* strain as the expression host. We also constructed a derivative modified in the translational initiation codon to ATG from TTG, designated as $_{TTG}$FDH and $_{ATG}$FDH. Membranes of the cells producing recombinant $_{TTG}$FDH and $_{ATG}$FDH showed approximately 20-times and 100-times higher specific activity than those of *G. japonicus* NBRC3260, respectively. The cells producing only FdhS and FdhL had no fructose oxidizing activity, but showed significantly high D-fructose:ferricyanide oxidoreductase activity in the soluble fraction of cell extracts,

whereas the cells producing the FDH complex showed activity in the membrane fraction. It is reasonable to conclude that the cytochrome *c* subunit is responsible not only for membrane anchoring but also for ubiquinone reduction.

Introduction

Fructose dehydrogenase (FDH; EC 1.1.99.11) of *Gluconobacter japonicus* NBRC3260 (formerly *Gluconobacter industrius* IFO3260), which catalyzes the oxidation of D-fructose to produce 5-keto-D-fructose, is a heterotrimeric membrane-bound enzyme with a molecular mass of ca. 140 kDa, consisting of subunits I (67 kDa), II (51 kDa), and III (20 kDa). The enzyme, purified for the first time in 1981, is a flavoprotein-cytochrome *c* complex, since subunits I and II have covalently bound flavin adenine dinucleotide (FAD) and heme C as prosthetic groups, respectively (1).

FDH shows strict substrate specificity to D-fructose, and thus, is used in diagnosis and food analysis and is commercially available (2). This enzyme is also used in a number of basic research projects to examine the electrochemical properties of enzyme-catalyzed electrode reactions, which is called bioelectrocatalysis (3). The reaction is classified into two types. One is the direct electron transfer (DET)-type system in which electrons are transferred directly between the enzyme and electrode. The other is the mediated electron transfer (MET)-type system in which mediators transfer electrons between the enzyme and electrode. As far as we know, FDH has the highest ability of DET-type bioelectrocatalysis on the anode (4). The DET-type system is convenient in the construction of compact bioelectrochemical devices, and is utilized to develop biosensors, biofuel cells, and bioreactors. However, DET-type bioelectrocatalysis occurs only at some limited kinds of

electrodes suitable for individual redox enzymes such as FDH (3), alcohol dehydrogenase (5), cellobiose dehydrogenase (6), bilirubin oxidase (7), and Cu efflux oxidase (8). Although DET-type bioelectrocatalysis is attractive for applications, mechanisms for the reaction have not been fully described yet. For the first step to explore the mechanisms of the DET-type bioelectrocatalytic reaction of FDH, we sequenced the genes encoding each subunit of the FDH complex from *G. japonicus* NBRC3260 and constructed an expression system to highly produce FDH in a *Gluconobacter oxydans* strain.

Materials and Methods

Materials

Fructose dehydrogenase of *Gluconobacter japonicus* NBRC3260 was both a gift from and purchased from Toyobo (Osaka, Japan). Restriction endonucleases and modification enzymes for genetic engineering were kind gifts from Toyobo (Osaka, Japan) and were also purchased from Takara Shuzo (Kyoto, Japan) and Agilent Technologies (Santa Clara, CA, USA). Yeast extract was a generous gift from Oriental Yeast (Osaka, Japan). All other materials were purchased from commercial sources of guaranteed grade.

Bacterial strains, plasmids, and growth conditions

The bacterial strains and plasmids used in this study are listed in Table 1. *Gluconobacter japonicus* NBRC3260 and *Gluconobacter oxydans* ATCC621H and NBRC12528 and its Δ*adhA*::Km^R derivative (9) were used in this study. The broad host range vector pBBR1MCS-4 was used for the heterologous expression of the *fdhSCL* genes in *G. oxydans*. *Gluconobacter* spp. were grown on ΔP medium, consisting of 5 g of glucose, 20 g of glycerol, 10 g of polypeptone, and 10 g of yeast extract per liter, at 30°C with vigorous shaking, unless otherwise stated. Kanamycin and ampicillin were used at final concentrations of 50 μg ml^{-1} and 250 μg ml^{-1}, respectively.

Escherichia coli DH5α was used for plasmid construction (10). *E. coli* HB101 harboring pRK2013 was used for a helper strain for conjugative plasmid transfer using a triparental mating method (11). *E. coli* strains were grown on modified Luria-Bertani medium, consisting of 10 g of polypeptone, 5 g of yeast extract, 5 g of NaCl, filled to 1 liter with distilled water, and adjusted pH to 7.0 with NaOH. Ampicillin was used at a final concentration of 50 μg ml^{-1}.

Determination of the N-terminal amino acid sequence of purified FDH

Commercially available FDH was subjected to SDS-PAGE (10% acrylamide). The proteins in the gel were transferred electrophoretically onto a polyvinylidene difluoride

membrane at 2 mA cm^{-2} for 40 min. Proteins were stained with CBB (Coomassie brilliant blue) stain one (Nacalai Tesque, Japan), destained with 5% (vol vol^{-1}) methanol, followed by the excision and drying of bands. The N-terminal amino acid sequence was analyzed with the peptide sequencer Procise 491 (Life Technologies, Carlsbad, CA, USA).

Sequencing of the *fdhSCL* genes

Degenerate primers, Forward primer A and Reverse primer B, were designed for PCR-based gene amplification (Table S1). The genomic DNA of *G. japonicus* was isolated from cells grown to a mid-exponential phase of growth by the method of Marmur (12) with some modifications, i.e. we used cetyltrimethylammonium bromide at a final concentration of 1% (wt vol^{-1}) to remove polysaccharides but omitted the perchlorate step in the original procedure. PCR was performed with the genomic DNA of *G. japonicus* as the parental DNA molecule using KOD Dash polymerase (Toyobo, Japan) and the MyCycler thermal cycler (Bio-Rad, CA, USA). The amplified DNA fragment was sequenced using the same primers. The thermal asymmetric interlaced PCR (TAIL-PCR) method was repeatedly conducted to extend sequencing to the 5' and 3' directions using one of the three arbitrary degenerate primers, AD1, AD2, or AD3, and KOD Dash polymerase, according to Liu et al. (13). The product of TAIL-PCR was sequenced to be homologous to the 3' region of the gene encoding the cytochrome *c* subunit of sorbitol dehydrogenase. Thus, degenerate

116 primers were designed from the conserved amino acid sequence in the heme C binding
117 motives in the cytochrome *c* subunits of other dehydrogenases to extend sequencing. We
118 repeated the TAIL-PCR method to further obtain the complete structural genes for the FDH
119 complex.
120

121 **Construction of plasmids**

122 For plasmid construction, we used Herculase II Fusion DNA polymerase (Agilent
123 Technologies, Santa Clara, CA, USA) to amplify the designed DNA fragments. A putative
124 promoter region of the *adhAB* genes, which encode two major subunits of the
125 pyrroloquinoline quinone-dependent alcohol dehydrogenase, was amplified with Herculase
126 II Fusion DNA polymerase using a genomic DNA preparation of *G. oxydans* 621H and two
127 primers, 621H-adh-pro(+) and 621H-adh-pro(-) (Table S1). The PCR product was inserted
128 into pBBR1MCS-4 (9) treated with *Kpn*I and *Xho*I to yield pSHO8. The *fdhSCL* genes
129 were amplified with the DNA polymerase using the genome DNA of *G. japonicus*
130 NBRC3260 and two primer sets, fdhS-5-Eco(+) and fdhL-3-PstBam(-) and
131 fdhS-370-ATG-Xho(+) and fdhL-3-PstBam(-) (Table S1), respectively. The PCR products
132 were inserted into pSHO8 treated with *Eco*RI and *Bam*HI and with *Xho*I and *Bam*HI to yield
133 pSHO12 and pSHO13, respectively. To construct a plasmid to express only the *fdhSL*
134 genes, an in-frame deletion in the *fdhC* gene was introduced in pSHO13 by fusion PCR as

follows. The 5' and 3' fragments for a deletion derivative of pSHO13, in which most of subunit II (from His^{11} to Trp^{451}, amino acid number of the putative mature subunit II) is lost in-frame, were amplified with the DNA polymerase with the primer sets of fdhS-370-ATG-Xho(+) and delta-fdhC(-) and delta-fdhC(+) and fdhL-3-PstBam(-), respectively (Table S1). The two PCR products were purified and conducted to fusion PCR with the primers fdhS-370-ATG-Xho(+) and fdhL-3-PstBam(-). The amplified 2.4-kb DNA fragment was inserted into pSHO8 treated with *Xho*I and *Bam*HI to yield pSHO16. All nucleotide sequences of PCR cloning were confirmed by cycle sequencing techniques using a 310 DNA sequencer (Applied Biosystems, CA, USA).

Expression of recombinant FDH and preparation of the membrane fraction

G. oxydans NBRC12528 Δ*adhA*::Km^R was transformed with the plasmids via a triparental mating method using the HB101 strain harboring pRK2013 (11). Acetic acid was added to the media for selection at a final concentration of 0.1% (wt vol^{-1}) to eliminate *E. coli* growth. Acetic acid- and ampicillin-resistant conjugant colonies were screened twice on ΔP agar medium containing 0.1% (wt vol^{-1}) acetic acid and 250 μg ml^{-1} ampicillin. Finally, the transconjugants were screened in liquid ΔP medium containing 250 μg ml^{-1} ampicillin.

Gluconobacter cells were cultivated in ΔP medium with or without 250 μg ml^{-1} ampicillin to the late exponential growth phase. Cells were collected by centrifugation at

10,000 *g* for 10 min and washed twice with 20-fold-diluted McIlvaine buffer (McB, mixture of 0.1 M citric acid and 0.2 M disodium hydrogenphosphate) (pH 6.0). Preparation of the membrane fraction was carried out as described by Ameyama et al. (1) with some modifications, as follows. Cells were suspended in 20-fold-diluted McB (pH 6.0) and were disrupted by two passages through a French pressure cell press (Thermo Fisher Scientific, Waltham, MA, USA). After cell debris was sedimented by low speed centrifugation (10,000 g, 10 min, 4°C), the supernatant was ultracentrifuged (100,000 g, 1 h, 4°C). The supernatant was used as the soluble fraction and precipitates were resuspended in 20-fold-diluted McB (pH 6.0) and used as the membrane fraction.

Purification of recombinant FDH

The solubilization and purification of FDH were performed as described (1) with some modifications, as follows. Membranes were suspended in 20-fold diluted McB (pH 6.0) at a concentration of 10 mg membrane protein ml^{-1} containing 1 mM 2-mercaptoethanol and 1.0% (wt vol^{-1}) Triton X-100 and gently stirred for 10 h at 4°C. FDH was obtained in the supernatant fraction of ultracentrifugation at 100,000 g for 1.5 h. The supernatant fraction was applied on a DEAE-sepharose column equilibrated with 20-fold diluted McB (pH 6.0) containing 1 mM 2-mercaptoethanol and 0.1% (wt vol^{-1}) Triton X-100. The elution of FDH from a DEAE-sepharose column was carried out by a concentration gradient of McB,

173 i.e. from 20-fold diluted McB (pH 6.0) to the original concentrations of McB (pH 6.0)
174 containing 1 mM 2-mercaptoethanol and 0.1% (wt vol^{-1}) Triton X-100. The purities of
175 recombinant FDH were judged by Coomassie brilliant blue R-250 staining of SDS-PAGE.
176

177 **Oxygen consumption rates by intact cells**

178 Oxygen consumption of intact *Gluconobacter* cells was measured at 25°C with a Clark-type
179 oxygen electrode (OPTO SCIENCE, Tokyo, Japan). Cell suspensions were prepared at
180 concentrations of 1.0 OD_{600nm} with 50 mM sodium phosphate buffer (pH 6.0). D-Glucose
181 and D-fructose were added at 200 mM as the respiration substrate. Oxygen concentrations
182 were recorded amperometrically as the reduction current of oxygen at -600 mV vs. the
183 Ag|AgCl reference electrode.
184

185 **Other analytical methods**

186 Global identity between predicted amino acid sequences was calculated by the software
187 GENETYX-MAC (ver. 14; GENETYX, Tokyo, Japan). Protein concentrations were
188 determined with the DC Protein Assay Kit (Bio-Rad, CA, USA) using bovine serum albumin
189 as a standard. FDH activity was measured spectrophotometrically with potassium
190 ferricyanide and the ferric-dupanol reagent as described (1). One FDH unit was defined as
191 the enzyme amount oxidizing one micromole of D-fructose per min. Covalently bound

heme C on protein separated by SDS-PAGE was stained by heme-catalyzed peroxidase activity (14). Heme C content was determined spectrophotometrically as described (15).

Nucleotide sequence accession number

The nucleotide sequence and their predicted amino acid sequence were deposited to the DNA data bank of Japan (DDBJ) with the accession number of AB728565.

Results

Sequencing of the *fdhSCL* genes

We determined the N-terminal amino acid sequence of subunit I of the commercially available FDH complex purified from *G. japonicus* NBRC3260 (*Gluconobacter* sp. in the instructions provided by Toyobo) to be SNETLSADVVIIGAGICGSLLAH (in an amino to carboxyl direction) as shown in Fig. S1. Basic Local Alignment Search Tool (BLAST) analysis of the determined amino acid sequence revealed that subunit I of sorbitol dehydrogenase (SLDH) of *Gluconobacter frateurii* THD32 shows the highest identity with the N-terminal amino acid sequence of subunit I of FDH (16). We thus designed degenerate primers for PCR (Table S1) based on the N-terminal sequence and conserved the

211 amino acid sequence in the SLDH subunit I, respectively. To obtain sequence information
212 upstream and downstream of the PCR product, the TAIL-PCR method was conducted as
213 described in the Materials and Methods section. We also designed degenerate primers from
214 the heme C binding consensus sequence, and further repeated the TAIL-PCR method. We
215 determined the nucleotide sequence of the 4,208-base PCR product containing the complete
216 structural genes for the FDH complex.

217 The nucleotide and predicted amino acid sequences of FDH and the flanking regions
218 are shown in Fig. S1. Three open reading frames (ORFs) were found for *fdhSCL* encoding
219 the small, cytochrome *c,* and large subunits, or subunit III, II, and I, respectively. They
220 may be in the same transcriptional unit. A sequence of SRRKLLA, similar to the
221 consensus motif SRRXFLK (where X is any polar amino acid) for the twin-arginine
222 translocation (tat) system of *E. coli* that translocates secretory proteins across the
223 cytoplasmic membrane, was found in the N terminus of FdhS (17). Since there was no
224 ATG or GTG codon between the tat signal and nonsense codon in the upstream region, a
225 TTG codon at nucleotide (nt) 93 can be the start codon for *fdhS*. A possible
226 Shine-Dalgarno sequence was found at 6-bp upstream of this start codon. We did not find a
227 rho-independent terminator-like sequence around the termination codon for *fdhL*, rather
228 there seems to have been another ORF from nt 3,794 of which the product is homologous to
229 the hypothetical protein GDI_0857 of *Gluconacetobacter diazotrophicus* PAI5 and the

hypothetical protein GMO_23960 of *Gluconobacter morbifer* G707. Since we failed to obtain the sequence for upstream and downstream regions of the *fdhSCL* genes, a whole structure of the *fdh* operon is uncertain. A 35-amino acid stretch in the predicted N terminus of subunit III can be recognized as a signal sequence by the SOSUIsignal program (18), whereas no signal sequence was found for the N terminus of subunit I, suggesting that subunit I may be translocated together with subunit III by the tat system. The *fdhS* gene encoded 183 amino acids but 148 for the mature protein, of which the calculated molecular mass was approx. 16 kDa.

The ORF corresponding to subunit II, *fdhC*, started at the position of nt 663. A possible SD sequence, AGGA, was found 15-nt upstream of the start codon. The 25 amino acid sequence of the predicted N terminus of FdhC was suggested as a sec-dependent signal sequence by the SOSUIsignal program (18). The molecular mass of the mature protein could be calculated as approx. 49 kDa composed of 461 amino acids, but it should be higher because the deduced amino acid sequence was revealed to have three CXXCH sequence motives for heme C binding sites.

The coding region of subunit I was started at position 2,145 with the ATG codon. There was a possible SD sequence, AGG, 9-nt upstream of the initiation codon. No signal sequence for translocation was found in the predicted sequence, consistent with the result of the N-terminal amino acid sequencing of purified FDH, which started at the second Ser

249 residue. The *fdhL* gene encoded a polypeptide of 544 amino acid residues with a calculated
250 molecular mass of approx. 60 kDa being assembled with and covalently bound to FAD.
251 The deduced amino acid sequence was found to have the GAGICG sequence at a position
252 between the 14th and 19th residues, corresponding to the binding motif of FAD (GXGXXG)
253 (19).

254 Global identity between the predicted amino acid sequences of each subunit of FDH
255 and SLDH from *G. frateurii* (16) was calculated as follows using the putative mature forms
256 of protein: subunit I, 52% identity; subunit II, 44% identity; subunit III, 24% identity. Even
257 though there are high identities, the SLDH of *Gluconobacter thailandicus* NBRC3254
258 (formally *Gluconobacter suboxydans* var. α IFO3254) closely related to that of *G. frateurii*
259 (16) has been shown to be inert on sugars but active on D-mannitol at only a 5% rate of
260 D-sorbitol (20). The global identity of each subunit of FDH with that of GDH from
261 *Burkholderia cepacia* (21) was 52%, 45%, and 32% for subunit I, subunit II, and subunit III,
262 respectively. *B. cepacia* GDH shows relatively wide substrate specificity, i.e. this enzyme
263 oxidizes maltose at half the rate of D-glucose (22). On the other hand, since thorough
264 substrate specificity has not been reported so far, it is not clear yet whether *B. cepacia* GDH
265 oxidizes other monosaccharides.

266 The putative mature form of the predicted amino acid sequence of *fdhC* showed
267 considerable identity to those of the cytochrome *c* subunits of ADH of *G. oxydans* (36%,

(23)) and aldehyde dehydrogenase of *Gluconacetobacter europaeus* (31%, (24)).

Construction of *Gluconobacter* strains for *fdhSCL* expression

Since *G. oxydans* NBRC12528 highly produces *c*-type cytochromes and flavoproteins (25) but does not have FDH activity (1), we tried heterologous expression of the *fdhSCL* genes in this strain. Moreover, because ADH is one of major membrane proteins in NBRC12528 and may disturb protein purification, its derivative, which has gene replacement in the *adhA* gene encoding a large subunit of ADH (Δ*adhA*::Km^R strain), was used in this study. The broad-host-range plasmid vector pBBR1MCS-4 was stable in *G. oxydans* NBRC12528 and easy to manipulate, thus we used this plasmid vector to express the *fdhSCL* genes. To ensure heterologous expression, a putative promoter region for the *adhAB* genes of *G. oxydans* 621H was inserted at the upstream region of the *fdhSCL* genes.

Judging from the multiple alignment analysis of subunit III of several flavoprotein-cytochrome *c* complex dehydrogenases (data not shown), the start codon of the FdhS subunit seemed to be TTG and not ATG. In addition to simple cloning of the native *fdhSCL* genes, in order to confirm the translational start site of subunit III and examine translation efficiency, we constructed modified *fdhSCL* genes to designate $fdh_{ATG}SCL$, where the TTG codon was replaced with ATG and a termination codon (TAA) was inserted just before the ATG codon. The Δ*adhA* strain was transformed with the constructed plasmids

287 by conjugation-based gene transfer.

288

289 **Comparison between wild-type and recombinant FDHs**

290 The *G. japonicus* NBRC3260 strain, which produces wild-type FDH, showed 0.15 FDH
291 units (mg membrane protein)$^{-1}$ in the membranes. Although we did not examine this in
292 detail, the low specific FDH activity in the membranes of *G. japonicus* NBRC3260 may be
293 attributed to the difference in the media used in the present and former studies, i.e. ΔP
294 medium was used in this study, while the former study used synthetic medium.
295 Membranes of the Δ*adhA* cells harboring pSHO12 carrying the wild-type *fdhSCL* genes
296 showed 3.5 ± 0.3 units mg^{-1}, activity approximately 20-times higher than those of *G.*
297 *japonicus* NBRC3260 (Fig. 1). Furthermore, those of $_{ATG}$FDH showed 16 ± 0.8 units mg^{-1},
298 approximately 5-times higher than $_{TTG}$FDH. We could not detect FDH activity in the
299 membranes of the Δ*adh* strain harboring pSHO8 carrying the putative promoter region only.
300 Heme-catalyzed peroxidase staining of the SDS-PAGE gel revealed that both
301 membranes having $_{TTG}$FDH and $_{ATG}$FDH showed approx. 51-kDa bands, while the Δ*adh*
302 strain harboring pSHO8 did not. The apparent intensity of staining of $_{ATG}$FDH was the
303 highest in the samples examined in this study, and that of $_{TTG}$FDH was also higher than that
304 of *G. japonicus* NBRC3260 (data not shown). These results clearly indicate that the
305 initiation codon for subunit III is TTG at nt 93, and also suggest that expressions of not only

306 subunit III, but also the whole FDH complex are increased by changing the initiation codon
307 to ATG.
308
309 **Characterization of purified $_{ATG}$FDH**
310 The specific activity of $_{ATG}$FDH purified in this study was 260 units (mg protein)$^{-1}$ at 25°C,
311 which is approx. 1.5-times higher than that reported in the previous study (1). The
312 purified $_{ATG}$FDH had three main bands of 68, 51, and 18 kDa on SDS-PAGE (Fig. S2),
313 which are similar sizes to those reported previously (1), and correspond with the expected
314 molecular masses from the *fdhSCL* genes determined in this study. At least two smaller
315 bands could be seen in the CBB-stained SDS-PAGE of our FDH preparation (Fig. S2).
316 However, we did not find these bands when we used other detergents for preliminary FDH
317 purification, such as n-dodecyl-β-D-maltoside and n-octyl-β-D-glucoside (S. Kawai, T.
318 Yakushi, K. Matsushita, and K. Kano, unpublished data). Thus, we likely consider them as
319 contaminants.
320 The purified $_{ATG}$FDH showed a reduced cytochrome *c*-like absorption spectrum
321 (data not shown), which is derived from the heme C moieties in subunit II. Based on the
322 FDH complex being a heterotrimeric structure, the number of heme C was determined to be
323 2.1 per complex, which was calculated from spectrometric heme C contents and protein
324 contents as described in the Materials and Methods section. We suggest that FDH has three

heme C moieties as predicted from the deduced amino acid sequence of subunit II, although the estimated value is more than two but much less than three, because some protein impurities can be seen in the CBB-stained SDS-PAGE of our FDH preparation (Fig. S2) and minor invisible contaminations are also possible.

The purified $_{ATG}$FDH transferred electrons to the electrodes directly, as commercially available FDH does (S. Kawai, T. Yakushi, K. Matsushita, and K. Kano, unpublished data).

Characterization of the subunit I/III subcomplex

To examine the roles of subunit II in the electron transfer to ubiquinone, the physiological electron acceptor, and ferricyanide, an artificial electron acceptor, and in the subcellular localization of the FDH complex, we constructed a strain to produce only subunits I and III. Oxygen consumption with D-glucose and D-fructose by the Δ*adhA* cells harboring pSHO8 (vector), pSHO13 (*fdh*$_{ATG}$*SCL*), or pSHO16 (*fdh*$_{ATG}$*SL*) were measured (Fig. 2). D-Fructose-dependent oxygen consumption by the Δ*adhA* cells harboring the empty vector was much lower than oxygen consumption with glucose by the same cells ($p < 0.01$, Student's *t* test; $n = 6$), suggesting that the Δ*adhA* strain and even the parental strain *G. oxydans* NBRC12528 have the glucose oxidizing respiratory chain as previously reported (26), but do not have the fructose oxidizing respiratory chain. They presumably have the

ability to metabolize D-fructose to produce NADH being re-oxidized by the respiratory chain. D-Glucose-dependent oxygen consumption rates by the Δ*adhA* cells harboring pSHO13 (*fdh*$_{ATG}$*SCL*) and pSHO16 (*fdh*$_{ATG}$*SL*) were increased by approx. 1.5-fold that of the cells harboring pSHO8 (vector) by a mechanism that has yet to be elucidated ($p < 0.01$, Student's *t* test; $n = 6$). The cells harboring pSHO13 (*fdh*$_{ATG}$*SCL*) showed the ability to consume oxygen depending on fructose at approx. a 10-fold faster rate than that of the cells harboring the empty vector ($p < 0.01$, Student's *t* test; $n = 6$), which is much higher than that observed with glucose, suggesting that the fructose-oxidizing respiratory chain was heterologously reconstituted in the Δ*adhA* cells. On the other hand, the difference in D-fructose-dependent oxygen consumption between the cells harboring pSHO16 (*fdh*$_{ATG}$*SL*) and those harboring the empty vector may be considered negligible ($p > 0.1$, Student's *t* test; $n = 6$).

In order to know whether the functional subunit I/III subcomplex is expressed, we examined the *in vitro* fructose dehydrogenase activity of the cell-free extract of the Δ*adhA* cells harboring pSHO16 (*fdh*$_{ATG}$*SL*). The activity of the cells that express whole FDH complex could be found mostly in the membrane fraction at a specific activity of 20 ± 5 units mg^{-1} at pH 5.0 (Fig. 3A). However, the activity of the cells that express the subunit I/III subcomplex (I/III) was detected mostly in the soluble fraction at a specific activity of 3.8 ± 0.4 units mg^{-1}, indicating that functional I/III is produced and subunit II is a membrane-anchoring subunit for the FDH complex. Because I/III had significant activity

363 to oxidize fructose but failed to link the respiratory chain, it is reasonable to conclude that
364 subunit II is responsible for ubiquinone reduction. By using the purified FDH complex and
365 partially purified I/III, we determined bimolecular rate constants for the reduction of several
366 artificial electron acceptors. I/III had no selectivity for electron acceptors, while the FDH
367 complex reacted specifically with 2,3-dimethoxy-5-methyl-1,4-benzoquinone (Q-0) and
368 2,3-dimethoxy-5-farnesyl-1,4-benzoquinone (Q-1) (S. Kawai, T. Yakushi, K. Matsushita,
369 and K. Kano, unpublished data). We examined the pH-dependency of fructose
370 dehydrogenase activity for the FDH complex in the membrane fraction and I/III in the
371 soluble fraction (Fig. 3B). They were different from each other, i.e. the optimum pH of the
372 FDH complex in the membrane fraction was pH 4.0, whereas I/III showed the highest
373 activity at pH 6.0.
374

375 ## Discussion

376 We purified the FDH complex from the membranes of *G. japonicus* NBRC3260 (formerly *G.*
377 *industrius* IFO3260) in 1981 (1). This enzyme is useful for the determination of D-fructose,
378 which can be applied in diagnosis (2), and more recently for basic research to understand the
379 properties of enzyme electrodes that can transfer electrons directly (3). Here, we sequenced
380 whole structural genes for the heterotrimeric complex for the first time. The genes for
381 several kinds of flavoprotein-cytochrome *c* complexes have been sequenced so far, such as

382 gluconate 2-dehydrogenase from *Erwinia cypripedii* (27), glucose dehydrogenase from *B.*
383 *cepacia* (BcGDH) (21), and sorbitol dehydrogenase from *G. frateurii* (16). Each enzyme
384 including FDH has strict substrate specificity, the genes determined in this study offer the
385 4th new member of the flavoprotein-cytochrome *c* complex family as fructose-specific
386 enzyme. Genes for 2-ketogluconate 5-dehydrogenase, a flavoprotein-cytochrome *c*
387 complex, still remain to be determined (28). The gene organization of the *fdh* genes is
388 unique to the others, i.e. the order of the genes is the small, large, and cytochrome *c* subunits
389 in the 5′ to 3′direction for those reported so far, whereas that of the *fdh* genes was the small,
390 cytochrome *c*, and large subunits. However, we anticipate that there is less physiological
391 significance for the difference in gene organization because we qualitatively reconstituted an
392 FDH complex from partially purified I/III and the cytochrome subunit independently
393 expressed (S. Kawai, T. Yakushi, K. Matsushita, and K. Kano, unpublished data). Another
394 unique feature predicted from the primary sequence of the FDH complex is a hydrophobic
395 patch in the C terminus of subunit II for integration into the membrane by a hydrophobic
396 helical structure, which can be predicted by a hydropathy plot using the SOSUI program (29)
397 (data not shown). However, we ran the secondary structure prediction program Jpred 3
398 (30), and the hydrophobic patch would be part of a sheet structure rather than helix with a
399 relatively high probability (data not shown). Thus, it is an interesting issue whether the
400 hydrophobic patch has a role in the membrane localization of subunit II or not.

We successfully overexpressed the FDH complex in the *G. oxydans* Δ*adhA* strain. This strain is beneficial for the expression of the heterologous protein in the host strain for purification because it fails to produce the ADH complex, one of the major membrane proteins in *Gluconobacter*. In addition, compared to *E. coli*, our expression system does not need to consider heme C assembly because *Gluconobacter* produces high amounts of *c*-type cytochromes naturally (25). Tsuya et al. reported on the heterologous expression of BcGDH in the *E. coli* strain harboring a plasmid to express the heme C assembly system (21). When pSHO13 ($fdh_{ATG}SCL$) was used, the membranes contained a specific FDH activity of 16 units mg^{-1}, suggesting that approx. 5% of the membrane proteins were the FDH complex, taking into account purified FDH, which had a specific activity of 260 units mg^{-1}. We suggest that *G. oxydans* can produce the FDH complex at such high productivity because it is a related species of *G. japonicus*.

The translation of subunit III was found to start at the TTG codon, by constructing the plasmid derivative pSHO13 ($fdh_{ATG}SCL$) containing a termination codon in-frame just before the initiation codon, which was substituted to the ATG codon. The *G. oxydans* strain harboring pSHO13 not only produced the FDH complex, but also a much higher amount of FDH. Translation initiation by the TTG codon is enhanced by the T signal (ATTT) in the 5' side of the initiation codon (31). However, we did not find a candidate for the T signal in the nucleotide sequence near the initiation codon. The results in this

420 study suggest that the TTG codon is a less efficient codon even in *Gluconobacter*, and its
421 substitution to the ATG codon improves translation efficiency.

422 Since we reconstituted the D-fructose oxidizing respiratory chain in *G. oxydans*
423 Δ*adhA* cells, we suggest that the FDH complex is a D-fructose:ubiquinone 5-oxidoreductase
424 functioning as the primary dehydrogenase in the respiratory chain of *G. japonicus*.
425 Moreover, the Δ*adhA* cells harboring pSHO16 ($fdh_{ATG}SL$) producing I/III only failed to
426 support the D-fructose oxidizing ability, even though these cells showed significantly high
427 D-fructose:ferricyanide oxidoreductase activity in the soluble fraction. Thus, we suggest
428 that subunit II is responsible for anchoring the FDH complex to the cytoplasmic membrane
429 and transferring electrons to ubiquinone. Another *Gluconobacter* membrane-bound
430 enzyme ADH consists of three subunits; one of which is a triheme cytochrome *c* subunit
431 (AdhB) responsible for ubiquinone reduction and membrane anchoring (32). The
432 cytochrome *c* subunit of heterotrimeric BcGDH has a functionally critical role in the
433 ubiquinone reaction and membrane localization (21). Indeed, a significant homology was
434 observed among FdhC, AdhB, and the β subunit of BcGDH (see the Results section). Our
435 results suggest an analogy of the cytochrome *c* function of other *Gluconobacter* enzymes
436 such as molybdopterin-dependent aldehyde dehydrogenase (24, 33) and other heterotrimeric
437 flavoprotein-cytochrome *c* complexes that can be found in many kinds of bacterial genomes.

438 As described earlier, the FDH complex was characterized by its ability to transfer

439 electrons to electrodes directly. As far as we know, this ability is unique to this enzyme
440 and details of the mechanisms remain unknown. We can start creating FDH derivatives
441 through genetic engineering procedures to characterize their electrochemical properties and
442 discuss the mechanism underlining direct electron transfer. Indeed, we observed large
443 differences in the pH-dependencies of the FDH complex and I/III (Fig. 3B). These findings
444 suggest that I/III has a different intramolecular electron transport pathway and different
445 electrochemical properties from the FDH complex.
446

447 Acknowledgements

448 We thank Yuichi Yoshino for his technical assistance. We are grateful to Osao Adachi
449 who continuously encourages us to proceed with our FDH study. This work was supported
450 in part by a Grant-in-Aid from the Japan Society for the Promotion of Science.
451

452 References

453 1. **Ameyama M, Shinagawa E, Matsushita K, Adachi O.** 1981. D-fructose
454 dehydrogenase of *Gluconobacter industrius*: purification, characterization, and
455 application to enzymatic microdetermination of D-fructose. J Bacteriol. **145:**814-823.

2. **Nakashima K, Takei H, Adachi O, Shinagawa E, Ameyama M.** 1985. Determination of seminal fructose using D-fructose dehydrogenase. Clin Chim Acta. **151:**307-310.

3. **Kamitaka Y, Tsujimura S, Kano K.** 2007. High current density bioelectrolysis of D-fructose at fructose dehydrogenase-adsorbed and Ketjen black-modified electrodes without a mediator. Chemistry Letters **36:**218-219.

4. **Kamitaka Y, Tsujimura S, Setoyama N, Kajino T, Kano K.** 2007. Fructose/dioxygen biofuel cell based on direct electron transfer-type bioelectrocatalysis. Phys Chem Chem Phys. **9:**1793-1801.

5. **Ikeda T, Kobayashi D, Matsushita F, Sagara T, Niki K.** 1993. Bioelectrocatalysis at electrodes coated with alcohol dehydrogenase, a quinohemoprotein with heme *c* serving as a built-in mediator. Journal of Electroanalytical Chemistry **361:**221-228.

6. **Gorton L, Lindgren A, Larsson T, Munteanu FD, Ruzgas T, Gazaryan I.** 1999. Direct electron transfer between heme-containing enzymes and electrodes as basis for third generation biosensors. Analytica Chimica Acta **400:**91-108.

7. **Tsujimura S, Nakagawa T, Kano K, Ikeda T.** 2004. Kinetic study of direct bioelectrocatalysis of dioxygen reduction with bilirubin oxidase at carbon electrodes. Electrochemistry **72:**437-439.

8. **Miura Y, Tsujimura S, Kamitaka Y, Kurose S, Kataoka K, Sakurai T, Kano K.** 2007. Bioelectrocatalytic reduction of O_2 catalyzed by CueO from *Escherichia coli* adsorbed on a highly oriented pyrolytic graphite electrode. Chemistry Letters **36:**132-133.

9. **Habe H, Shimada Y, Yakushi T, Hattori H, Ano Y, Fukuoka T, Kitamoto D, Itagaki M, Watanabe K, Yanagishita H, Matsushita K, Sakaki K.** 2009. Microbial production of glyceric acid, an organic acid that can be mass produced from glycerol. Appl Environ Microbiol. **75:**7760-7766.

10. **Grant SG, Jessee J, Bloom FR, Hanahan D.** 1990. Differential plasmid rescue from transgenic mouse DNAs into *Escherichia coli* methylation-restriction mutants. Proc Natl Acad Sci U S A. **87:**4645-4649.

11. **Figurski DH, Helinski DR.** 1979. Replication of an origin-containing derivative of plasmid RK2 dependent on a plasmid function provided in trans. Proc Natl Acad Sci U S A. **76:**1648-1652.

12. **Marmur J.** 1963. A procedure for the isolation of deoxyribonucleic acid from microorganisms. Methods in Enzymology **6:**726-738.

13. **Liu YG, Mitsukawa N, Oosumi T, Whittier RF.** 1995. Efficient isolation and mapping of *Arabidopsis thaliana* T-DNA insert junctions by thermal asymmetric interlaced PCR. Plant J. **8:**457-463.

14. **Goodhew CF, Brown KR, Pettigrew GW.** 1986. Haem staining in gels, a useful tool in the study of bacterial *c*-type cytochromes. Biochimica et Biophysica Acta **852:**288-294.

15. **Berry EA, Trumpower BL.** 1987. Simultaneous determination of hemes *a*, *b*, and *c* from pyridine hemochrome spectra. Anal Biochem. **161:**1-15.

16. **Toyama H, Soemphol W, Moonmangmee D, Adachi O, Matsushita K.** 2005. Molecular properties of membrane-bound FAD-containing D-sorbitol dehydrogenase from thermotolerant *Gluconobacter frateurii* isolated from Thailand. Biosci Biotechnol Biochem. **69:**1120-1129.

17. **Berks BC, Palmer T, Sargent F.** 2005. Protein targeting by the bacterial twin-arginine translocation (Tat) pathway. Curr Opin Microbiol. **8:**174-181.

18. **Gomi M, Sonoyama M, Mitaku S.** 2004. High performance system for signal peptide prediction: SOSUIsignal. Chem-Bio Informatics Journal **4:**142-147.

19. **Dym O, Eisenberg D.** 2001. Sequence-structure analysis of FAD-containing proteins. Protein Sci. **10:**1712-1728.

20. **Shinagawa E, Matsushita K, Adachi O, Ameyama M.** 1982. Purification and characterization of D-sorbitol dehydrogenase from membrane of *Gluconobacter suboxydans* var. α. Agricultural and Biological Chemistry **46:**135-141.

21. **Tsuya T, Ferri S, Fujikawa M, Yamaoka H, Sode K.** 2006. Cloning and functional expression of glucose dehydrogenase complex of *Burkholderia cepacia* in *Escherichia coli*. J Biotechnol. **123:**127-136.

22. **Yamaoka H, Yamashita Y, Ferri S, Sode K.** 2008. Site directed mutagenesis studies of FAD-dependent glucose dehydrogenase catalytic subunit of *Burkholderia cepacia*. Biotechnol Lett. **30:**1967-1972.

23. **Kondo K, Horinouchi S.** 1997. Characterization of the genes encoding the three-component membrane-bound alcohol dehydrogenase from *Gluconobacter suboxydans* and their expression in *Acetobacter pasteurianus*. Appl Environ Microbiol. **63:**1131-1138.

24. **Thurner C, Vela C, Thony-Meyer L, Meile L, Teuber M.** 1997. Biochemical and genetic characterization of the acetaldehyde dehydrogenase complex from *Acetobacter europaeus*. Arch Microbiol. **168:**81-91.

25. **Matsushita K, Toyama H, Adachi O.** 1994. Respiratory chains and bioenergetics of acetic acid bacteria. Adv Microb Physiol. **36:**247-301.

26. **Matsushita K, Shinagawa E, Adachi O, Ameyama M.** 1989. Reactivity with ubiquinone of quinoprotein D-glucose dehydrogenase from *Gluconobacter suboxydans*. J Biochem. **105:**633-637.

27. **Yum DY, Lee YP, Pan JG.** 1997. Cloning and expression of a gene cluster encoding three subunits of membrane-bound gluconate dehydrogenase from *Erwinia cypripedii* ATCC 29267 in *Escherichia coli*. J Bacteriol. **179:**6566-6572.

28. **Shinagawa E, Matsushita K, Adachi O, Ameyama M.** 1981. Purification and characterization of 2-keto-D-gluconate dehydrogenase from *Gluconobacter melanogenus*. Agricultural and Biological Chemistry **45:**1079-1085.

29. **Hirokawa T, Boon-Chieng S, Mitaku S.** 1998. SOSUI: classification and secondary structure prediction system for membrane proteins. Bioinformatics. **14:**378-379.

30. **Cole C, Barber JD, Barton GJ.** 2008. The Jpred 3 secondary structure prediction server. Nucleic Acids Res. **36:**W197-201.

31. **Ganoza MC, Marliere P, Kofoid EC, Louis BG.** 1985. Initiator tRNA may recognize more than the initiation codon in mRNA: a model for translational initiation. Proc Natl Acad Sci U S A. **82:**4587-4591.

32. **Matsushita K, Yakushi T, Toyama H, Shinagawa E, Adachi O.** 1996. Function of multiple heme *c* moieties in intramolecular electron transport and ubiquinone reduction in the quinohemoprotein alcohol dehydrogenase-cytochrome *c* complex of *Gluconobacter suboxydans*. J Biol Chem. **271:**4850-4857.

546 33. **Adachi O, Tayama K, Shinagawa E, Matsushita K, Ameyama M.** 1980.
547 Purification and characterization of membrane-bound aldehyde dehydrogenase from
548 *Gluconobacter suboxydans*. Agricultural and Biological Chemistry **44:**503-515.
549 34. **Boyer HW, Roulland-Dussoix D.** 1969. A complementation analysis of the
550 restriction and modification of DNA in *Escherichia coli*. J Mol Biol. **41:**459-472.
551 35. **Kovach ME, Elzer PH, Hill DS, Robertson GT, Farris MA, Roop RM, 2nd,**
552 **Peterson KM.** 1995. Four new derivatives of the broad-host-range cloning vector
553 pBBR1MCS, carrying different antibiotic-resistance cassettes. Gene. **166:**175-176.

554

555 **Figure legends**

556 Fig. 1. Comparison of specific FDH activity in the membranes of *G. japonicus* NBRC3260
557 (wild type) and the Δ*adhA* strains harboring pSHO8 (vector), pSHO12 (native *fdhSCL*), or
558 pSHO13 ($fdh_{ATG}SCL$). Data are shown as mean values with 90% confidence intervals
559 (error bars; $n = 3$).

560

561 Fig. 2. D-Fructose-dependent oxygen consumption (heavy gray columns) of the whole cell
562 preparations of the Δ*adhA* strains harboring pSHO8 (vector), pSHO13 ($fdh_{ATG}SCL$), or
563 pSHO16 ($fdh_{ATG}SL$). Control experiments were also conducted with D-glucose (light gray
564 columns). The rates of oxygen consumption were normalized by optical density of the cell

565 preparations. Data are shown as mean values with 90% confidence intervals (error bars; *n*
566 = 3). Significance can be seen between columns with a and b, a and c, and c and d ($p <$
567 0.01, Student's *t* test; $n = 6$). Columns with the same letters were not significantly different
568 ($p > 0.1$, Student's *t* test; $n = 6$).

569

570 Fig. 3. Comparison of the FDH complex (FDH) and I/III. (A) The membrane (light gray
571 columns) and soluble (heavy gray columns) fractions of the Δ*adhA* strains harboring pSHO8
572 (vector), pSHO13 ($fdh_{ATG}SCL$), or pSHO16 ($fdh_{ATG}SL$) were prepared, and FDH activity in
573 the membrane and soluble fractions were measured at pH 5.0 and pH 6.0, respectively.
574 Total activity in each fraction was shown. (B) FDH activities of the membrane fraction for
575 the FDH complex and the soluble fraction for I/III were measured under various pH
576 conditions. Relative activity to that of the highest activity was shown individually. Data
577 are shown as mean values with 90% confidence intervals (error bars; $n = 3$). The specific
578 FDH activities of the membrane fraction of the cells harboring pSHO13 ($fdh_{ATG}SCL$) and the
579 soluble fraction of the cells harboring pSHO16 ($fdh_{ATG}SL$) were 20 ± 5 and 3.8 ± 0.4 units
580 mg^{-1}, respectively.

581

582

582 Table 1. The bacterial strains and plasmids used in this study.

Strains and plasmids	Description	Source or reference
Bacterial strains		
Escherichia coli		
DH5α	F$^-$ *endA1 hsdRJ7* (r_k^-, m_k^+) *supE44 thi-1* λ$^-$ *recAl gyrA96 relA1 deoR* Δ(*lacZYA-argF*)U169 ϕ80d*lacZ*ΔM15	(10)
HB101	F$^-$ *thi-1 hsdS20* (r_B, m_B) *supE44 recA13 ara14 leuB6 proA2 lacY1 galK2 rpsL20* (str^r *xyl-5 mtl-1* λ$^-$)	(34)
Gluconobacter japonicus		
NBRC3260	Wild type	NBRC[a]
Gluconobacter oxydans		
NBRC12528	Wild type	NBRC[a]
Δ*adhA*	NBRC12528 Δ*adhA*::Km^R	(9)
ATCC621H	Wild type	ATCC[a]
Plasmids		
pKR2013	The plasmid mediates plasmid transfer, Km^R	(11)
pBBR1MCS-4	A broad host range plasmid, *mob* Ap^R	(35)
pSHO8	pBBR1MCS-4, a 0.7-kb fragment of a putative promoter region of the *adhAB* gene of *G. oxydans* 621H	This study
pSHO12	pSHO8, a 3.8-kb fragment of the *fdhSCL* genes of *G. japonicus* NBRC3260	This study
pSHO13	pSHO8, a 3.7-kb fragment of the *fdh*$_{ATG}$*SCL* genes	This study
pSHO16	pSHO8, a 2.4-kb fragment of the *fdh*$_{ATG}$*SL* genes (in-frame deletion of *fdhC*)	This study

583 [a], The URL addresses of NBRC and ATCC are "http://www.nbrc.nite.go.jp/" and

584 "http://www.atcc.org/", respectively.

585

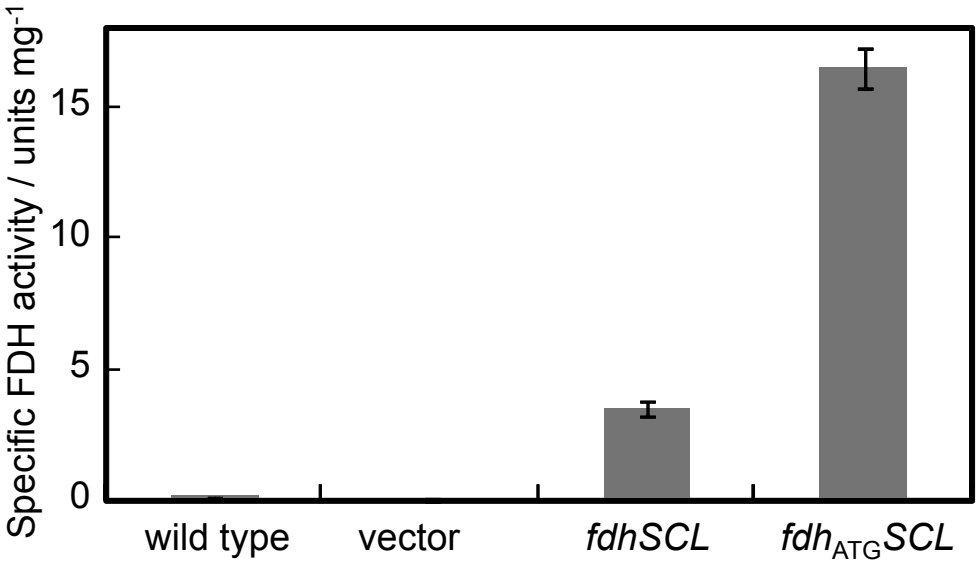

Kawai et al.

Fig. 1. Comparison of specific FDH activity in the membranes of *G. japonicus* NBRC3260 (wild type) and the Δ*adh* strains harboring pSHO8 (vector), pSHO12 (native *fdhSCL*), or pSHO13 ($fdh_{ATG}SCL$). Data are shown as mean values with 90% confidence intervals (error bars; n = 3).

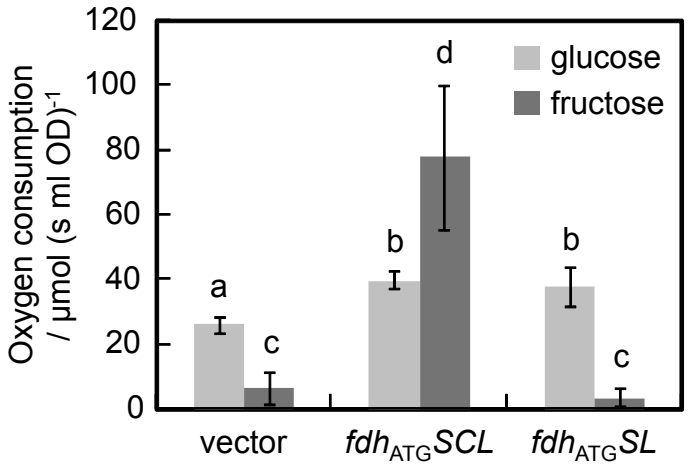

Kawai et al.

Fig. 2. D-Fructose-dependent oxygen consumption (heavy gray columns) of the whole cell preparations of the Δ*adh* strains harboring either pSHO8 (vector), pSHO13 (*fdh*$_{ATG}$*SCL*), or pSHO16 (*fdh*$_{ATG}$*SL*). Control experiments were also conducted with D-glucose (light gray columns). The rates of oxygen consumption were normalized by optical density of the cell preparations. Data are shown as mean values with 90% confidence intervals (error bars; $n = 3$). Significance can be seen between columns with a and b, a and c, and c and d ($p < 0.01$, Student's t test; $n = 6$). Columns with the same letters were not significantly different ($p > 0.1$, Student's t test; $n = 6$).

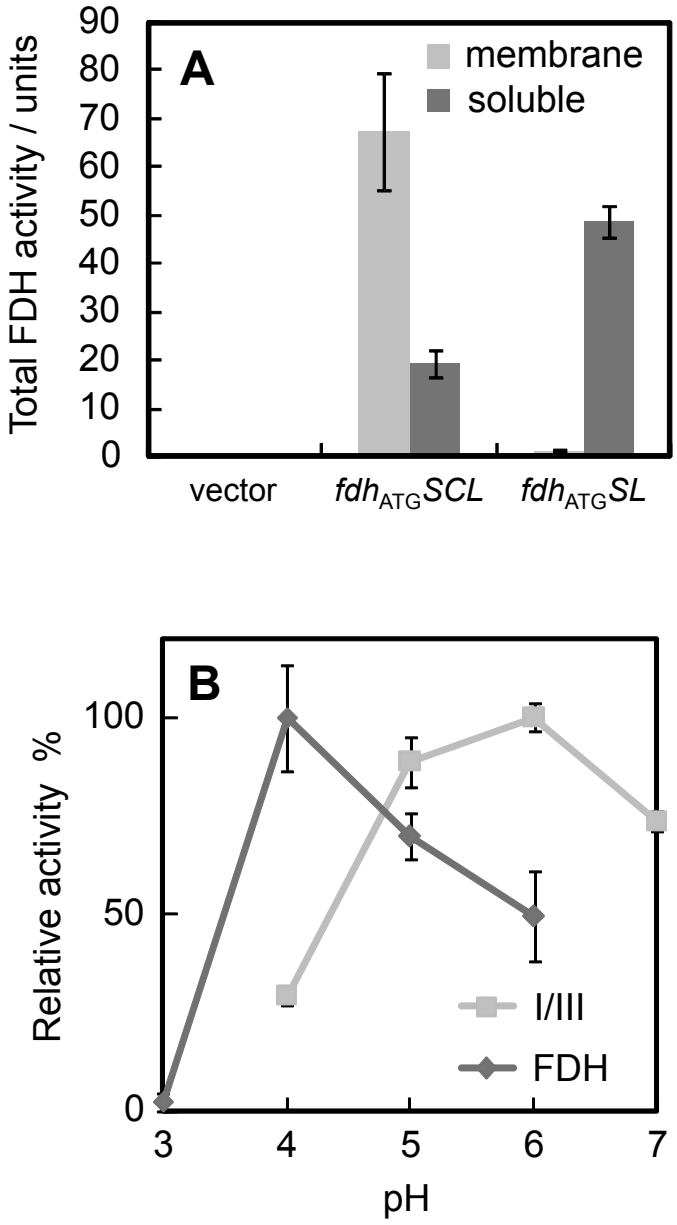

Kawai et al.

Fig. 3. Comparison of the FDH complex (FDH) and I/III. (A) The membrane (light gray columns) and soluble (heavy gray columns) fractions of the Δ*adhA* strains harboring pSHO8 (vector), pSHO13 (*fdh*$_{ATG}$*SCL*), or pSHO16 (*fdh*$_{ATG}$*SL*) were prepared, and FDH activity in the membrane and soluble fractions were measured at pH 5.0 and pH 6.0, respectively. Total activity in each fraction was shown. (B) FDH activities of the membrane fraction for the FDH complex (heavy gray diamonds) and the soluble fraction for I/III (light gray squares) were measured under various pH conditions. Relative activity to that of the highest activity was shown individually. Data are shown as mean values with 90% confidence intervals (error bars; n = 3). The specific FDH activities of the membrane fraction of the cells harboring pSHO13 (*fdh*$_{ATG}$*SCL*) and the soluble fraction of the cells harboring pSHO16 (*fdh*$_{ATG}$*SL*) were 20 ± 5 and 3.8 ± 0.4 units mg^{-1}, respectively.

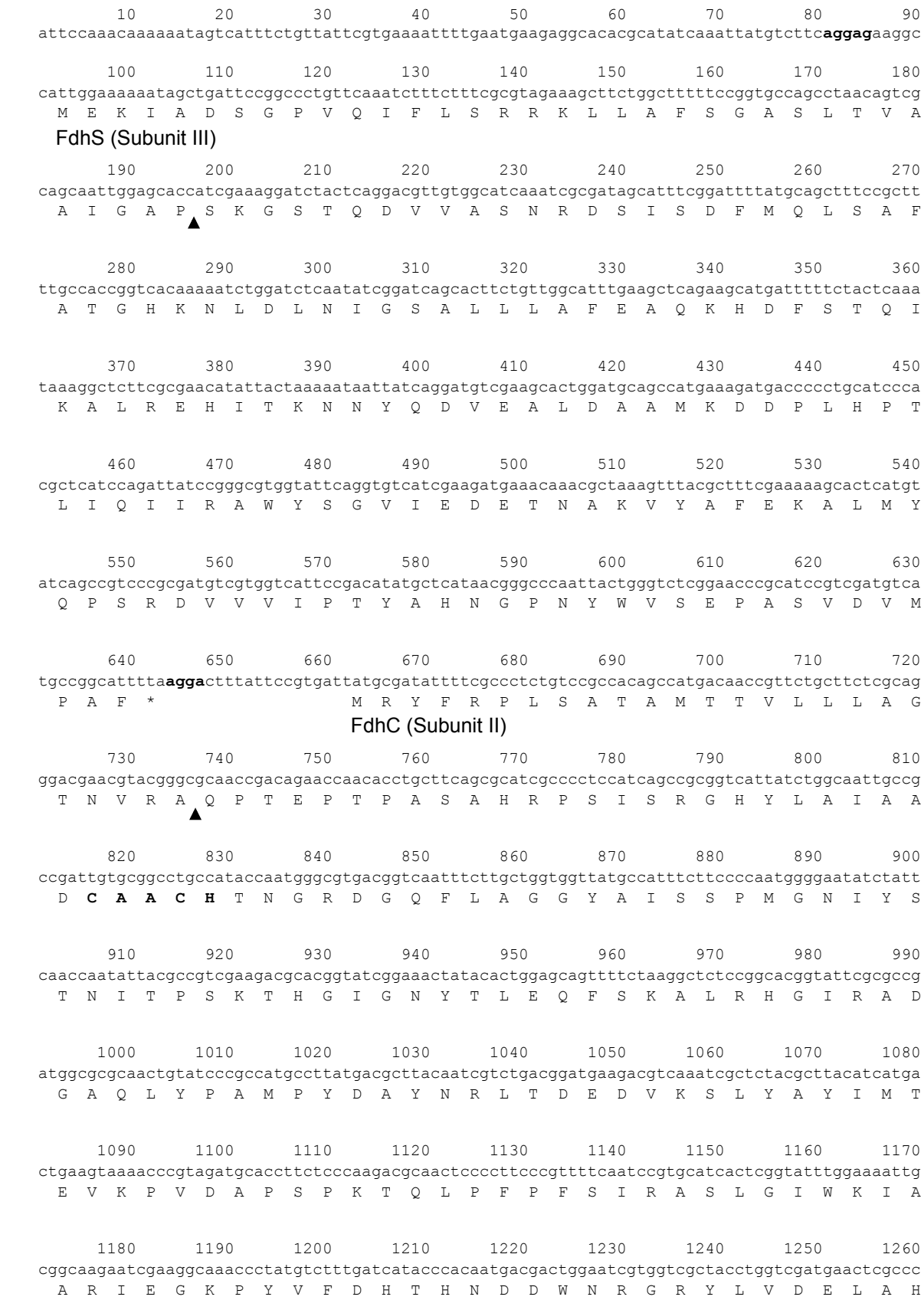

Kawai et al., Fig. S1 (continued).

```
     1270      1280      1290      1300      1310      1320      1330      1340      1350
attgtggagagtgtcacacaccgcgtaactttcttctagcgcccaatcagtccgcttatcttgctggtgcggacataggatcatggcgtg
  C  G  E  C  H  T  P  R  N  F  L  L  A  P  N  Q  S  A  Y  L  A  G  A  D  I  G  S  W  R  A

     1360      1370      1380      1390      1400      1410      1420      1430      1440
caccaaatattaccaatgcccctcaaagcggtattggcagttggtcggatcaggatctcttccaatatctgaaaactggaaaaaccgcac
  P  N  I  T  N  A  P  Q  S  G  I  G  S  W  S  D  Q  D  L  F  Q  Y  L  K  T  G  K  T  A  H

     1450      1460      1470      1480      1490      1500      1510      1520      1530
atgctcgtgcagcaggaccaatggcagaagcaatcgagcatagcctacaatatcttccggatgccgatatttctgccatagttacatatc
  A  R  A  A  G  P  M  A  E  A  I  E  H  S  L  Q  Y  L  P  D  A  D  I  S  A  I  V  T  Y  L

     1540      1550      1560      1570      1580      1590      1600      1610      1620
ttcgttcggttccggcaaaggcagaaagcggtcaaacagtcgctaattttgagcatgccggccgcccatccagttacagtgttgctaacg
  R  S  V  P  A  K  A  E  S  G  Q  T  V  A  N  F  E  H  A  G  R  P  S  S  Y  S  V  A  N  A

     1630      1640      1650      1660      1670      1680      1690      1700      1710
ctaactcccgtcgcagcaatagtactctgacaaaaacaaccgatggtgctgcactctacgaggctgtgtgcgccagttgccatcaatctg
  N  S  R  R  S  N  S  T  L  T  K  T  T  D  G  A  A  L  Y  E  A  V  C  A  S  C  H  Q  S  D

     1720      1730      1740      1750      1760      1770      1780      1790      1800
acggtaaagggtccaaagacggttattatccttccctcgtaggaaatacgacgaccgggcaactcaatccaaatgatctgatcgccagta
  G  K  G  S  K  D  G  Y  Y  P  S  L  V  G  N  T  T  T  G  Q  L  N  P  N  D  L  I  A  S  I

     1810      1820      1830      1840      1850      1860      1870      1880      1890
ttctttacggtgtggaccgcacaacggataaccacgaaatcctgatgccggcttttggtccagactctctcgtacagcccctgacagatg
  L  Y  G  V  D  R  T  T  D  N  H  E  I  L  M  P  A  F  G  P  D  S  L  V  Q  P  L  T  D  E

     1900      1910      1920      1930      1940      1950      1960      1970      1980
agcagatcgccacaatcgcggactacgttctaagccactttggcaatgcccaggccacagtctcggcagatgcggtcaaacaggtgcggg
  Q  I  A  T  I  A  D  Y  V  L  S  H  F  G  N  A  Q  A  T  V  S  A  D  A  V  K  Q  V  R  A

     1990      2000      2010      2020      2030      2040      2050      2060      2070
cgggcggaaagcaggttcctctcgccaagctcgccagtccgggcgtgatgctgcttctcggaactggtggcatcctgggagccattctgg
  G  G  K  Q  V  P  L  A  K  L  A  S  P  G  V  M  L  L  L  G  T  G  G  I  L  G  A  I  L  V

     2080      2090      2100      2110      2120      2130      2140      2150      2160
tggtagccggcctctggtggctgatcagccgtcgcaaaaagcgttccgcttaataagattcaaggtcaaaatcatgtctaatgaaacgc
  V  A  G  L  W  W  L  I  S  R  R  K  K  R  S  A  *                   M  S  N  E  T  L
                                                                                FdhL (Subunit I)

     2170      2180      2190      2200      2210      2220      2230      2240      2250
tttcggctgatgtcgtcatcattggagcaggaatctgcggctccctgctcgcccacaaactcgtccgcaacggactttctgtgctgctcc
  S  A  D  V  V  I  I  G  A  G  I  C  G  S  L  L  A  H  K  L  V  R  N  G  L  S  V  L  L  L

     2260      2270      2280      2290      2300      2310      2320      2330      2340
tggatgcaggtccccgccgggaccgctcccagatcgtagaaaactggcggaacatgccgcctgacaacaagtcccagtacgattatgcaa
  D  A  G  P  R  R  D  R  S  Q  I  V  E  N  W  R  N  M  P  P  D  N  K  S  Q  Y  D  Y  A  T

     2350      2360      2370      2380      2390      2400      2410      2420      2430
caccttaccccagcgtaccctgggccccgcataccaactacttcccagacaataactacctgattgtcaaaggcccggaccggacggctt
  P  Y  P  S  V  P  W  A  P  H  T  N  Y  F  P  D  N  N  Y  L  I  V  K  G  P  D  R  T  A  Y
```

Kawai et al., Fig. S1 (continued).

```
      2440      2450      2460      2470      2480      2490      2500      2510      2520
acaagcaaggaatcatcaaaggcgtcgggggtacaacctggcactgggcggcttcaagctggcggtacctgcccaacgatttcaagctgc
  K  Q  G  I  I  K  G  V  G  G  T  T  W  H  W  A  A  S  S  W  R  Y  L  P  N  D  F  K  L  H

      2530      2540      2550      2560      2570      2580      2590      2600      2610
attccacatatggcgtgggccgcgattacgccatgagctacgacgaacttgagccttactattacgaggccgagtgcgaaatgggcgtga
  S  T  Y  G  V  G  R  D  Y  A  M  S  Y  D  E  L  E  P  Y  Y  Y  E  A  E  C  E  M  G  V  M

      2620      2630      2640      2650      2660      2670      2680      2690      2700
tgggaccaaacggcgaagagattacaccgtctgcgcctcgccaaaatccatggccgatgacctccatgccttacggatatggagaccgca
  G  P  N  G  E  E  I  T  P  S  A  P  R  Q  N  P  W  P  M  T  S  M  P  Y  G  Y  G  D  R  T

      2710      2720      2730      2740      2750      2760      2770      2780      2790
ctttcacggagatcgtcagcaagctcggtttctcaaacactcctgttccgcaggcacggaacagtcgtccttatgatggccgaccacaat
  F  T  E  I  V  S  K  L  G  F  S  N  T  P  V  P  Q  A  R  N  S  R  P  Y  D  G  R  P  Q  C

      2800      2810      2820      2830      2840      2850      2860      2870      2880
gctgtggcaacaacaactgcatgccaatctgcccgattggcgcgatgtacaatggcgtatacgcggcaataaaagcggaaaagctgggcg
  C  G  N  N  N  C  M  P  I  C  P  I  G  A  M  Y  N  G  V  Y  A  A  I  K  A  E  K  L  G  A

      2890      2900      2910      2920      2930      2940      2950      2960      2970
caaaaattattcccaatgctgtcgtctatgcgatggaaacggatgcaaaaaaccggatcacagcgattagcttctatgatcccgacaagc
  K  I  I  P  N  A  V  V  Y  A  M  E  T  D  A  K  N  R  I  T  A  I  S  F  Y  D  P  D  K  Q

      2980      2990      3000      3010      3020      3030      3040      3050      3060
agtcccatcgcgtcgttgcaaaaacatttgtgatcgccgcaaacgggatcgaaacaccgaaactgctgcttctggcggcaaatgatcgaa
  S  H  R  V  V  A  K  T  F  V  I  A  A  N  G  I  E  T  P  K  L  L  L  L  A  A  N  D  R  N

      3070      3080      3090      3100      3110      3120      3130      3140      3150
accctcatgggattgccaactcatcagaccttgttggccggaacatgatggaccatccgggcatcggcatgagcttccagtctgcggagc
  P  H  G  I  A  N  S  S  D  L  V  G  R  N  M  M  D  H  P  G  I  G  M  S  F  Q  S  A  E  P

      3160      3170      3180      3190      3200      3210      3220      3230      3240
ccatctgggctggtggaggctcagtccagatgagttccatcaccaacttccgtgatggcgatttccgctcggagtatgctgccacgcaga
  I  W  A  G  G  G  S  V  Q  M  S  S  I  T  N  F  R  D  G  D  F  R  S  E  Y  A  A  T  Q  I

      3250      3260      3270      3280      3290      3300      3310      3320      3330
tcggctacaacaatacggcccagaactcacgcgccggcatgaaagctctgtccatggggttggttggcaagaagctggatgaagaaatcc
  G  Y  N  N  T  A  Q  N  S  R  A  G  M  K  A  L  S  M  G  L  V  G  K  K  L  D  E  E  I  R

      3340      3350      3360      3370      3380      3390      3400      3410      3420
gccgtcgtacggcgcatggtgtggacatttatgccaaccatgaagtcctcccggaccccaacaaccgtcttgttctctccaaagactata
  R  R  T  A  H  G  V  D  I  Y  A  N  H  E  V  L  P  D  P  N  N  R  L  V  L  S  K  D  Y  K

      3430      3440      3450      3460      3470      3480      3490      3500      3510
aggatgcgctcggtattccacatcctgaagtcacctacgatgttggggagtatgttcggaagtcagctgccatctcaagacagcgcctga
  D  A  L  G  I  P  H  P  E  V  T  Y  D  V  G  E  Y  V  R  K  S  A  A  I  S  R  Q  R  L  M

      3520      3530      3540      3550      3560      3570      3580      3590      3600
tggatatcgccaaagccatgggcggtacggaaatcgagatgactccgtattttacgcccaacaaccacatcaccggtggcactatcatgg
  D  I  A  K  A  M  G  G  T  E  I  E  M  T  P  Y  F  T  P  N  N  H  I  T  G  G  T  I  M  G
```

Kawai et al., Fig. S1 (continued).

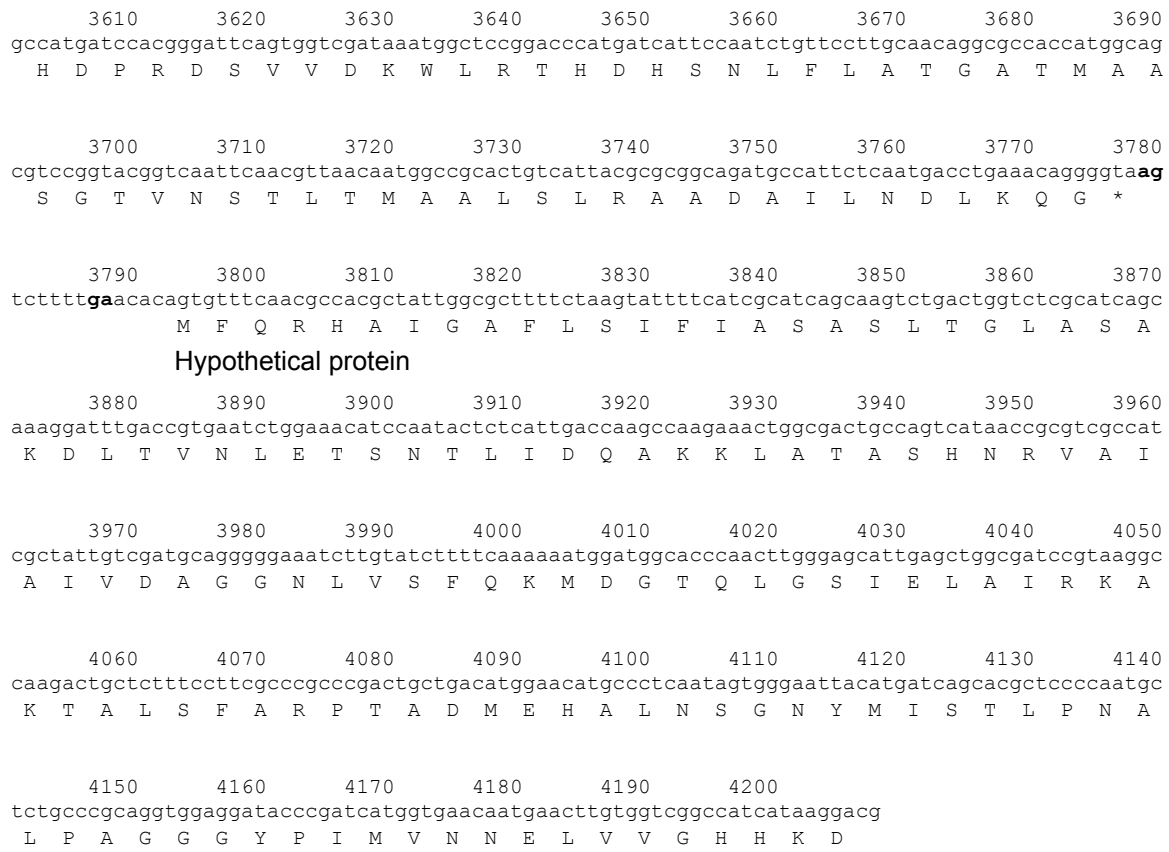

Kawai et al.

Fig. S1. Nucleotide and predicted amino acid sequences of *fdhSCL* are shown. Part of the gene for a hypothetical protein downstream of *fdhL* is also shown. Possible ribosome-binding sites located prior to the initiation codon of each gene are shown in bold face. Consensus sequences for heme C binding and FAD binding are shown in bold face. Black arrowheads indicate putative cleavage sites for the precursor forms of subunits II and III, predicted by the SOSUIsignal program. The amino acid sequence of subunit I determined by the peptide sequencer is underlined. The nucleotide sequence and predicted amino acid sequences for *fdhSCL* were deposited to DDBJ with the accession number AB728565.

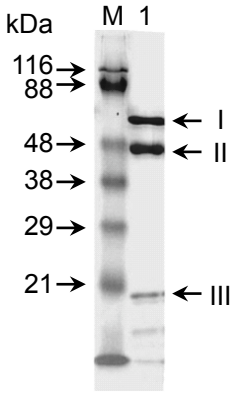

Kawai et al.

Fig. S2. Coomassie staining of the purified FDH complex separated by SDS-PAGE. Lane M, Molecular mass standard and 10 μg of the purified FDH complex were applied on lanes 1 and M, respectively.

Table S1. Oligonucleotides used in this study.

Primer name	Sequence (5´ --> 3´)[a]	Objective
Forward primer A	CSGCCGAYGTCGTGATYATYGGTG	Degenerate PCR and sequencing
Reverse primer B	GGCARATCGGCATRCARTTRTTRTTNCC	Degenerate PCR and sequencing
AD1	NTCGASTWTSGWGTT	TAIL-PCR
AD2	NGTCGASWGANAWGAA	TAIL-PCR
AD3	WGTGNAGWANCANAGA	TAIL-PCR
621H-adh-pro(+)	GGGGTACCTTCTGGCGGTACGGAGTC[b]	pSHO8
621H-adh-pro(-)	CCGCTCGAGATTAACCAGAAGTCATGATCCAAC[b]	pSHO8
fdhS-5-Eco(+)	GAATTCCAAACAAAAAATAGTC[b]	pSHO12
fdhL-3-PstBam(-)	GGATCCTGCAGCGTGGCGTTGAAACACTG[b]	pSHO12
fdhS-370-ATG-Xho(+)	CTCGAGGAGAAGGTAAATGGAAAAAATAGCTGATTC[b]	pSHO13
delta-fdhC(+)	gaaccaacacctgcttcagcgCTGATCAGCCGTCGCAAAAAG[c]	pSHO16
delta-fdhC(-)	CTTTTTGCGACGGCTGATCAGcgctgaagcaggtgttggttc[c]	pSHO16

[a], N = A, C, G, or T; R = A or G; Y = C or T.

[b], The engineered endonuclease recognition site is underlined.

[c], The 3' and 5' regions of *fdhC* are shown in lower and upper cases, respectively.